JOC The Journal of Organic Chemistry

pubs.acs.org/joc Note

Radical SAM Enzyme QmpB Installs Two 9-Membered Ring Sactionine Macrocycles during Biogenesis of a Ribosomal Peptide Natural Product

Alessio Caruso and Mohammad R. Seyedsayamdost*

Cite This: J. Org. Chem. 2021, 86, 11284–11289 Read Online

ACCESS | Metrics & More | Article Recommendations | Supporting Information

ABSTRACT: We report the reaction catalyzed by QmpB, a new radical *S*-adenosylmethionine enzyme encoded by a ribosomal peptide natural product gene cluster in *Streptococcus suis*. Using isotopic labeling, site-directed mutagenesis, high-resolution mass spectrometry, and multidimensional NMR spectroscopy, we show that QmpB installs two 9-membered ring sactionine bridges, connecting a Cys residue with an upstream Asn via an α-thioether bridge, with the two macrocycles separated by a single residue. QmpB is only the second type II sactionine synthase characterized to date.

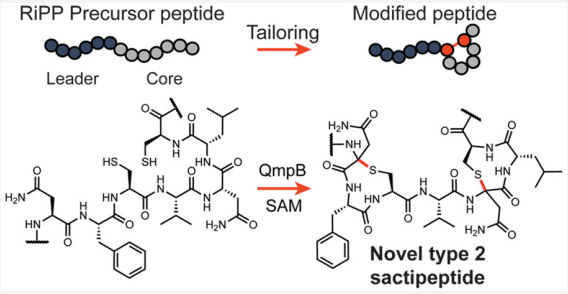

Downloaded via BROAD INST on June 28, 2022 at 02:09:32 (UTC).
See https://pubs.acs.org/sharingguidelines for options on how to legitimately share published articles.

Ribosomally synthesized and post-translationally modified peptides (RiPPs) have emerged as a structurally diverse family of natural products with a range of biological activities.[1] The production of RiPPs is based on a straightforward biosynthetic logic in which a short precursor peptide is produced ribosomally, then modified in the core region of the peptide by tailoring enzymes, and usually trimmed at the final step before secretion of the mature product (Figure 1A). RiPPs are defined by the types of modifications in the core peptide region. The characterization of modification enzymes, therefore, is essential in the identification of new RiPP subfamilies. We recently reported the structure and biosynthesis of streptide, a structurally unique RiPP with an unusual carbon−carbon cross-link between the side chains of lysine and tryptophan, which is installed by a radical *S*-adenosylmethionine (RaS) metalloenzyme.[2,3] The RaS enzyme superfamily is the largest in Nature, with over 600000 annotated members of which only a small fraction has been characterized.[4] The catalytic prowess of this superfamily relies on formation of the highly oxidizing 5′-deoxyadenosyl radical, which typically initiates turnover via abstraction of a substrate hydrogen atom. We surmised that in the context of RiPP biogenesis, this versatile enzyme family could deliver unprecedented transformations, thereby affording novel natural product scaffolds, as seen in streptide. To test our hypothesis, we searched for RiPP biosynthetic gene clusters (BGCs) that are modified by RaS enzymes, a subclass that has become known as RaS-RiPPs.[5] We anchored the search with two features: the presence of at least one RaS enzyme-encoding gene as well as a nearby *shp/rgg* quorum sensing (QS) system,[6] reasoning that the resulting natural products would be novel, owing to the versatility of RaS enzymes, and physiologically important, as QS is a key virulence determinant in numerous pathogens.[6] The search yielded ∼600 unique BGCs, which grouped into 16 distinct subfamilies of RaS-RiPPs when organized by precursor peptide homology (Figure 1B).[5] Our subsequent mining of the RaS-RiPPs network has shown it to be a rich source of novel enzymatic transformations and natural products, which include a tetrahydrobenzindole modification in tryglysins,[5,7] α- and β-thioether bonds in streptosactin and the *NxxC* subfamily,[8,9] respectively, an α-ether bridge in the *TQQ* subfamily,[10] as well as a new arginine-tyrosine C−C bond in *RRR* (Figure 1B).[11] The present study sought to elucidate the reaction of another uncharacterized group of RaS enzymes, the *QMP* subfamily that is predominantly encoded in the pathogen *Streptococcus suis*.

The *qmp* gene cluster from *S. suis* is controlled by an *shp/rgg* QS operon and encodes a precursor peptide (QmpA), a RaS enzyme (QmpB), and a combination protease-export protein (QmpC, Figure 1C). To characterize the reaction of QmpB, we pursued an *in vitro* biochemical approach in which we would prepare QmpA using solid-phase peptide synthesis (SPPS) and monitor its reaction with recombinant QmpB using chromatography-coupled high-resolution mass spectrometry (HR-MS), tandem HR-MS (HR-MS/MS), and multidimensional NMR spectroscopy (Table S1).

Special Issue: Natural Products: An Era of Discovery in Organic Chemistry

Received: June 26, 2021
Published: August 5, 2021

ACS Publications © 2021 American Chemical Society

https://doi.org/10.1021/acs.joc.1c01507
J. Org. Chem. 2021, 86, 11284−11289

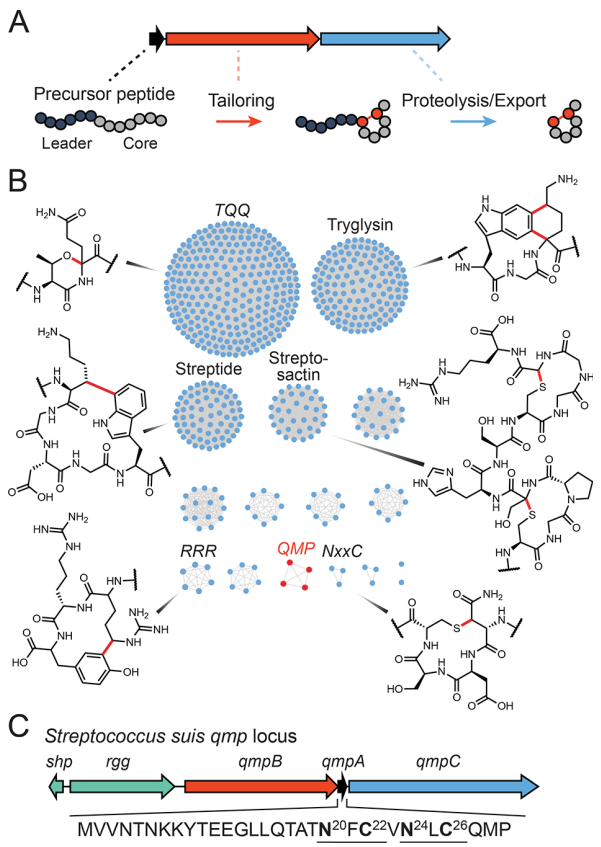

Figure 1. (A) General biosynthetic logic of RiPP natural products. (B) Sequence similarity network of streptococcal RaS-RiPP BGCs that are regulated by an *shp*/*rgg* QS operon. Structures of RaS enzyme-catalyzed modifications are shown with newly installed bonds rendered in red. The *qmp* family explored in this work is highlighted. (C) *qmp* BGC from *S. suis* YS56. Genes are color coded as follows: *shp*/*rgg* QS operon (green), RaS enzyme (red), precursor peptide (black), and transporter (blue). The sequence of the precursor peptide QmpA is shown.

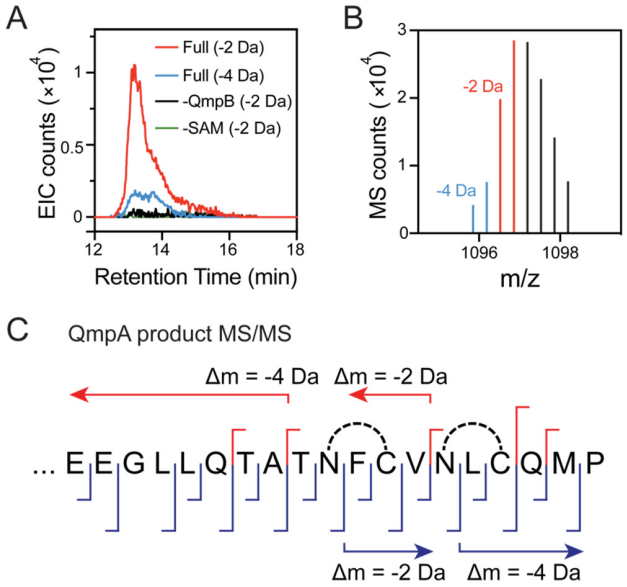

Figure 2. HR-MS analysis of modified QmpA after reaction with QmpB. (A) Extracted ion chromatogram of the QmpB products. In the full reaction, the −2 Da (red) and −4 Da (blue) products can be detected. For reactions lacking QmpB (black) or SAM (green), neither the −2 Da nor the −4 Da product can be observed; extracted ion traces for the −2 Da products are shown for these control reactions. (B) Mass spectrum of QmpB products. Masses corresponding to −2 Da (red), −4 Da (blue), and masses overlapping with unmodified QmpA (black) are highlighted. Note that the spectrum of the triply charged peptide is shown (see Table S2). (C) HR-MS/MS analysis of wt QmpA after reaction with QmpB. Fragment ions are displayed by blue (b-ions) and red (y-ions) dividers (see Table S3). The mass loss associated with modifications is highlighted in each direction of fragmentation, and the macrocycles are represented by black arcs.

The 29mer QmpA was prepared by SPPS using standard methods and subsequently purified to homogeneity (see Table S2 for HR-MS data). QmpB was cloned as a hexaHis-tagged construct and expressed in *E. coli*. Anaerobic purification of QmpB resulted in protein featuring a typical RaS enzyme UV−vis spectrum (Figure S1), including absorption features at 320 and 400 nm that are symptomatic for [4Fe-4S] clusters.[12] Quantification of Fe and labile sulfide following reconstitution via standard methods revealed 8.7 ± 0.4 Fe(II) and 3.2 ± 0.4 S^{2-} per protomer, reflecting partial insertion of Fe−S clusters.[12] The high Fe(II) content is consistent with the bioinformatic prediction of additional binding site(s) for Fe−S clusters in the *C*-terminal SPASM domain of QmpB (Figure S2).[13]

Typical for active RaS enzymes, QmpB gave rise to time-dependent formation of 5′-deoxyadenosine in the absence of substrate (Figure S3), suggesting that our preparation of QmpB is competent in reductive cleavage of the cofactor *S*-adenosylmethionine (SAM). Next, upon incubation of synthetic QmpA with QmpB, SAM, and reductant ($Na_2S_2O_4$) under anaerobic conditions, we observed formation of a major species that was 2 Da lighter than substrate, as well as a minor species with a mass loss of 4 Da in ∼5:1 ratio (Figure 2A,B, Table S2). These were only observed in the presence of all components, but not when SAM or QmpB were omitted from the reaction, consistent with their assignment as reaction products (Figure 2A). Targeted HR-MS/MS provided initial insights into the structure of modified QmpA. Because the two product peaks overlapped chromatographically, HR-MS/MS was carried out with the −4 Da species, revealing that y fragment ions were unaltered relative to substrate downstream of C26, −2 Da relative to substrate between N24 and N20, and −4 Da upstream of N20 (Figure 2C, Table S3). Analogously, the b ion fragments were unaltered relative to substrate upstream of N20, −2 Da relative to substrate between N20 and N24, and −4 Da downstream of N26. These patterns are consistent with cross-link formation between N20−C22 and N24−C26 in QmpA. Observation of collision-induced dissociation within the macrocycle is in line with an α-thioether bridge (Figure 2C), as opposed to β-thioether bonds, which are more stable and do not fragment under typical ESI-MS conditions.[14] As further verification, we conducted HR-MS/MS analysis with the recently reported Asn-Cys β-thioether bridge installed by NxxcB (Figure 1B).[9] Identical HR-MS/MS conditions, which fragmented within the Asn-Cys macrocycle in the QmpB product, did not result in any detectable fragments internal to the macrocycle generated by NxxcB product (Figure S4), thereby providing further evidence that the QmpB-installed cross-links are α-thioethers.

To definitively elucidate the nature of the thioether bridge, we synthesized an isotopologue of QmpA containing uniformly ^{13}C-labeled Asn (^{13}C-Asn-QmpA) at both cross-linking positions, N20 and N24 (Table S2). Upon treatment of ^{13}C-Asn-QmpA with QmpB, SAM, and reductant, we observed

https://doi.org/10.1021/acs.joc.1c01507
J. Org. Chem. 2021, 86, 11284−11289

approximately 40% conversion of substrate to product (Figure S5). The product again consisted of a major −2 Da component and a minor −4 Da fraction in a ∼ 4:1 ratio. HR-MS data were consistent with two Asn-Cys macrocycles, as with the unlabeled QmpA substrate (Table S2). Importantly, 1D/2D NMR spectral analysis allowed us to assign the α-thioether cross-link correlations upon comparison with NMR data obtained with the unreacted QmpA substrate (Figure 3A, Figures S6 and S7).

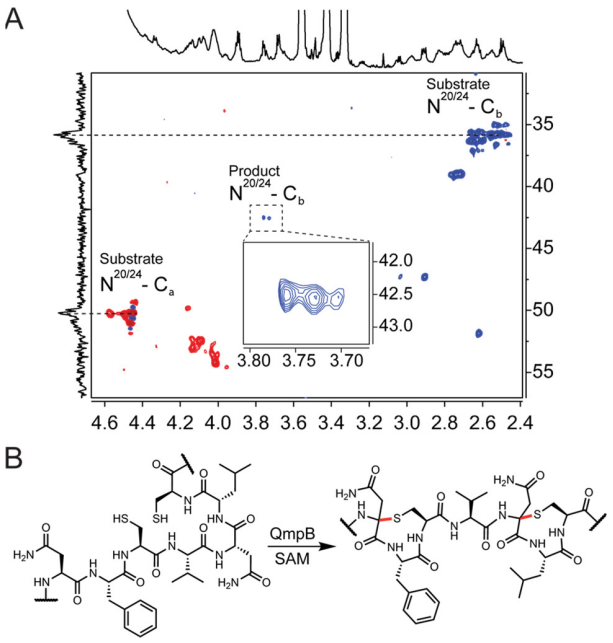

Figure 3. Structural characterization of the QmpB product. (A) DEPT-edited HSQC spectrum of ^{13}C-QmpA substrate/product mixture following after reaction with QmpB (red, CH/CH$_3$; blue, CH$_2$). The unmodified ^{13}C-Asn ("substrate") correlations are indicated with dashed lines. The product ^{13}C-Asn crosspeak ("product") is boxed. The inset shows a magnified view of the key Cβ/Hβ methylene in the α-thioetherified product. (B) Reaction catalyzed by QmpB. The two QmpB-installed α-thioether linkages are shown in red.

Most notably, unreacted QmpA exhibited Cα/Hα and Cβ/Hβ chemical shifts at N20/N24 of ∼50.3/4.45 and ∼35.8/2.55 ppm, respectively (Figure S6). Upon reaction with QmpB, the Cβ/Hβ pair remained as a methylene unit, as indicated by a DEPT-edited HSQC spectrum and was now significantly downshifted to ∼42.5/3.74 ppm (Figure 3A), consistent with the presence of a thioether linkage at the α-carbon.[9,15] This correlation was absent in the substate (Figure S6). These results mark QmpB as a sactionine synthase (Figure 3B), the family of RaS enzymes that install α-thioether bonds in several RiPPs, including subtilosin A and the sporulation killing factor (SKF).[15,16] The 9-membered ring macrocycles with a single intervening residue installed by QmpB are unusually small; in all sactipeptides identified to date, these can range from 12−84-membered macrocycles, that is, typically consisting of 2−26 intervening residues.[15] The absolute configuration of the cross-linked Cα in modified QmpA remains to be determined.

With the structure of the QmpB product established, we probed the directionality of QmpB catalysis using site-directed QmpA mutants, Cys22Ser- and Cys26Ser-QmpA, which were prepared via SPPS (Table S2). Each peptide was reacted with QmpB, SAM, and reductant. We observed enzyme-dependent formation of a −2 Da product from both substrates in approximately 20−40% yield (Figure 4A). HR-MS and HR-MS/MS analysis indicated formation of a singly cross-linked product involving the remaining Cys residue and the corresponding Asn two residues upstream (Figure 4B, Tables S2, S4, and S5). The observation of singly cyclized products with both substrate variants suggests that QmpB does not install the two macrocycles in a strictly specific order, unlike the sactionine synthase GggB involved in the production of streptosactin.[9] Rather, each site can serve as a substrate to QmpB, consistent with the double conserved amino acid motif of −N-Φ-C− in QmpA, where Φ represents a hydrophobic residue (Figure 1C).

In summary, we have elucidated the reaction carried out by an additional RaS enzyme in our network of RaS-RiPPs from mammalian microbiome streptococci. Sactionine linkages are the key defining feature of sactipeptides, and this family of RiPP natural products comes in two forms: Type 1 sactipeptides contain a nested topology in which the Cys residues and the corresponding acceptor residues are located *N*-terminally and *C*-terminally, respectively; this arrangement is observed in subtilosin A and thurincin H (Figure 4C).[15] In contrast, type 2 sactipeptides, exemplified by the founding member streptosactin, contain alternating Cys and acceptor residues, resulting in a sequential, unnested sactionine topology (Figure 4C).[9] From our studies above, we conclude that QmpB is a type 2 sactionine synthase that installs two small three-residue macrocycles using sactionine bridges. It is only the second example of this type of modification. QmpB differs from the type 2 sactisynthase GggB in that it does not install the two macrocycles in a specific order. Moreover, the directionality of the modifications is reversed (Figure 4C). Upon modification of QmpA by QmpB, the peptide is likely trimmed to remove the leader sequence and deliver the mature product for which we propose the name suisactin. We surmise that suisactin contains two sactionine bridges, and that the observation of singly cross-linked QmpA is due to incompletely reconstituted QmpB as indicated by the quantification of Fe and labile S^{2-}. A modification to the standard reconstitution procedure or alternative methods with different reductants and/or protein redox partners could lead to higher Fe−S cluster content. Future studies could also explore *S. suis* for the detection of suisactin and subsequently its biological activity. The latter aspect will be intriguing as the streptococcal RaS-RiPPs investigated so far have revealed narrow-spectrum antimicrobial, and possibly fratricidal, bioactivities.[7,9]

EXPERIMENTAL SECTION

Materials and Strains. All materials were purchased from Sigma-Aldrich or Fisher Scientific unless otherwise specified. Restriction enzymes, T4 DNA ligase, proof-reading Q5 High-Fidelity DNA Polymerase, Shrimp Alkaline Phosphatase, and Trypsin-Ultra (Mass Spectrometry grade) and the corresponding buffers were purchased from New England BioLabs (NEB). DNA oligos were purchased from Genewiz. PCR reactions were routinely carried out in Failsafe buffer D (Epicenter). All Fmoc- and side chain-protected amino acids and other components for solid-phase peptide synthesis were purchased from Millipore Sigma except for HATU and HOAt, which were obtained from GenScript. Low-loading 2-chlorotrityl chloride ProTide (Cl-TCP Cl ProTide) resin was purchased from CEM. Uniformly ^{13}C/^{15}N-labeled L-Asn was purchased from Cambridge Isotope Laboratories.

General Procedures. UV−vis absorption spectra were acquired on a Cary 60 UV−vis spectrophotometer (Agilent). Low-resolution high-performance liquid chromatography−mass spectrometry (HPLC−MS) analysis was performed on an Agilent instrument consisting of a

https://doi.org/10.1021/acs.joc.1c01507
J. Org. Chem. 2021, 86, 11284−11289

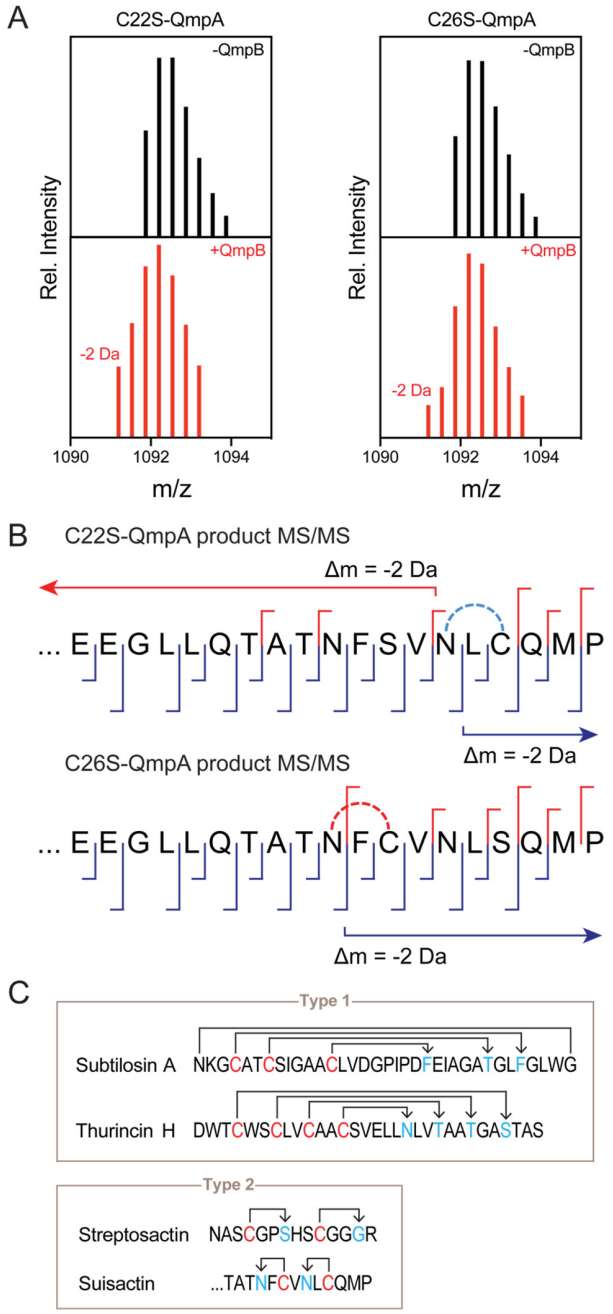

Figure 4. C22S- and C26S-QmpA are accepted by QmpB. (A) Mass spectra of C22S-QmpA (left) and C26S-QmpA (right) before and after reaction with QmpB, SAM, and $Na_2S_2O_4$. The triply ionized mass envelope is shown. (B) HR-MS/MS analysis of Cys-to-Ser QmpA mutants after reaction with QmpB. Fragment ions are displayed by blue (b-ions) and red (y-ions) dividers (see Tables S4 and S5). In both cases, the remaining unmodified cysteine is accepted by QmpB and cross-linked to the Asn two residues upstream. (C) Topologies of type 1 and 2 sactipeptides. The nested type 1 sactipeptide topology is formed from N-terminal Cys and C-terminal acceptor residues; subtilosin A and thurincin H are shown as examples. QmpB generates the rare type 2 sactipeptide topology upon reaction with QmpA, resulting in unnested thioether cross-links and only the second reported example of this topology.

liquid autosampler, a 1260 Infinity Series HPLC system combined with a diode array detector, and a 6120 Series ESI mass spectrometer. Samples were resolved on a Phenomenex Luna C18 column (3 μm, 4.6 mm × 100 mm) at a flow rate of 0.75 mL/min with the following elution parameters: 5% MeCN in water for 2 min, 5−100% MeCN over 10 min, and finally an isocratic 100% MeCN over 3 min. HPLC solvents contained 0.1% (v/v) formic acid (FA).

High-resolution (HR) HPLC−MS and HR-tandem-MS were carried out on an Agilent 6540 Accurate-Mass quadrupole time-of-flight (Qtof) instrument, consisting of a 1260 Infinity Series HPLC system, an automated liquid sampler, a diode array detector, a JetStream ESI source, and the 6540 Series Qtof. Samples were resolved on a reversed phase Phenomenex Luna C18 column (3 μm, 100 × 4.6 mm). The mobile phase consisted of water and MeCN (+0.1% FA). Elution was carried out as follows: 5% MeCN in water for 2 min followed by a gradient of 5−90% MeCN over 10 min, and finally 90%−100% MeCN over 4 min, at a flow rate of 0.75 mL/min.

Additionally, HR ultraperformance liquid chromatography-MS (HR-UPLC−MS) and HR-tandem UPLC-MS were carried out on an Agilent 6546 Accurate-Mass Qtof instrument consisting of a 1290 Infinity Series HPLC system, an automated liquid sampler, a diode array detector, a dual JetStream ESI source, and the 6546 Series Qtof. UPLC−MS samples were resolved on a reversed phase Agilent Poroshell EC C18 UPLC column (2.7 μm, 50 × 3 mm). The mobile phase consisted of water and MeCN (+0.1% formic acid). Elution was carried out with a gradient of 10−90% MeCN over 2.5 min, and then 90%−100% MeCN over 0.5 min, at a flow rate of 0.5 mL/min.

HPLC purifications were carried out on an Agilent 1260 Infinity Series analytical or preparative HPLC system equipped with a temperature-controlled column compartment, a diode array detector, and an automated fraction collector. The analytical system was also equipped with an automated liquid sampler. Nuclear magnetic resonance (NMR) spectra were acquired at the Princeton University Department of Chemistry Facilities. NMR spectra were collected in the triple resonance cryoprobe of a Bruker Avance III HD 800 MHz NMR spectrometer. The ^{13}C-QmpA peptide samples were prepared in 200 mM ammonium bicarbonate buffer in D_2O in a 2.5 mm diameter tube. 1D/2D NMR data—specifically ^{13}C, ^{1}H, and distortionless enhancement by polarization transfer (DEPT)-edited heteronuclear single quantum coherence (HSQC) data—were analyzed with MestReNova software.

Cloning of *S. suis* QmpB. Codon-optimized *qmpB* DNA fragments were obtained from Genewiz and designed to have 20 bp overlap regions with digested pET-28b(+) to allow for HiFi assembly using the NEB Mastermix. The *qmpB* fragment and pET-28b(+) were digested with NdeI/XhoI and the fragments purified using the Qiagen Gel Extraction Kit. The linearized vector was treated with Shrimp Alkaline Phosphatase (rSAP) prior to HiFi DNA assembly, which was carried out according to manufacturer instructions. Chemically competent *E. coli* DH5α cells were transformed with 2 μL of the HiFi ligation mixture by heat-shock and plated onto LB-agar plates containing 50 μg/mL kanamycin. The final assembled plasmids were confirmed by Sanger sequencing.

Expression, Purification, and Reconstitution of QmpB. Expression, purification, and reconstitution of QmpB was carried out using previously published procedures with slight modifications.[12] Cells were grown in M9 minimal media with $FeCl_3$ as an iron source, which was added to a final concentration of 50 μM immediately after IPTG induction (0.5 mM final IPTG concentration), when cultures reached an optical density at 600 nm (OD600) of ∼0.6. The cultures were incubated at 18 °C/120 rpm overnight. They were then spun down (8000*g*, 15 min, 4C) and frozen. Twenty-eight grams of cell paste was obtained from 10 L culture. QmpB was purified under anoxic conditions using published methods without modifications, yielding ∼11 mg of pure QmpB from 13.4 g cell paste.[12] Purified QmpB was quantified using the method reported by Barr et al.[12b] QmpB was anaerobically reconstituted with 10-fold excess Fe(II) and 10- fold excess Na_2S, as per reported procedures.[4] Iron and labile sulfide quantification was then carried out using prior procedures.[12]

Synthesis of QmpA Peptides. QmpA, ^{13}C-QmpA, C22S-QmpA, and C26S-QmpA were prepared by Fmoc-based SPPS on a Cl-TCP-Cl ProTide-resin using a Liberty Blue automated peptide synthesizer

https://doi.org/10.1021/acs.joc.1c01507
J. Org. Chem. 2021, 86, 11284−11289

equipped with a Discover microwave module (CEM). The deprotection solution consisted of 10% piperazine (w/v) in a 10:90 solution of EtOH/NMP (*N*-methylpyrrolidine) supplemented with 0.1 M HOBt (1-hydroxybenzotriazole). The activator solution consisted of 0.25 M DIC (*N*,*N*′-diisopropylcarbodiimide) in DMF and activator base solution of 0.5 M ethyl cyanohydroxyiminoacetate with 0.1 M *N*,*N*-diisopropylethylamine in DMF. A typical coupling cycle used 5 equiv of amino acid and 5 equiv of coupling reagent. Residues 1−4, 16, 22, 26, and 27 were double-coupled. The synthesis was typically performed on a 50 μmol scale, except for the $^{13}C_4$,$^{15}N_2$−N20/N24-QmpA (for simplicity, denoted as ^{13}C-QmpA) which was carried out on a 25 μmol scale. Upon completion of the synthesis, the resin was removed from the reaction vessel and transferred to an Econo-Pac column (BioRad). The resin was washed several times with DMF, followed by DCM, and dried thoroughly under vacuum. Peptide was cleaved from the resin by incubation with freshly prepared cleavage cocktail for 3 h at room temperature (5 mL per 100 mg resin) consisting of 90% TFA, 2.5% H_2O, 2.5% TIS (triisopropylsilane), and 5% βME (2-mercaptoethanol). The mixture was drained from the reaction tube and the resin was washed several times with TFA. The filtrate and washes were then combined and concentrated by evaporation of TFA under a stream of N_2. The peptide was then precipitated by addition of 10 volumes of ice-cold diethyl ether and isolated by centrifugation (4000*g*, 10 min, 4 °C). The ether was poured off, and the peptide was dried over a stream of N_2.

Purification of QmpA. Dried QmpA was dissolved in 40% MeCN with 100 mM ammonium bicarbonate and purified by preparative or semipreparative HPLC. Larger scale syntheses were injected onto a preparative Phenomenex C18 column (7 μm, 2.5 × 25 cm), which was equilibrated in 10% MeCN in H_2O (+0.1% FA). The peptide was eluted with a gradient of 10−70% MeCN over 20 min. The purity of QmpA was verified by HR-HPLC−MS and NMR analysis (see Table S2 and Figure S6). Smaller scale syntheses were instead injected onto a Synergi Fusion-RP semipreparative column (4 μm, 10 × 250 mm) and purified with the same elution protocol.

Enzymatic Activity Assays. Enzymatic assays were performed in an inert atmosphere within an MBraun glovebox. The various QmpA peptides were transported into the glovebox as prealiquoted lyophilized material and dissolved directly in the purified QmpB solution. Sodium dithionite (DT), DTT, and *S*-adenosylmethionine (SAM) were also transported into the glovebox as powders and prepared as stock solutions in water inside the box. Reactions were typically carried out in 0.5 mL Eppendorf tubes on a 30 μL scale with final concentrations of 2.5 mM DTT, 2.5 mM DT, 0.25 mM substrate peptide, 25 μM QmpB, and 1 mM SAM. Incubation time was typically 16 h. At the end of the incubation period, the reaction tubes were quenched by the addition of 1 volume of MeCN and a final concentration of 200 mM ammonium bicarbonate. The precipitate following quenching was spun down at 21,000g for 5 min and the supernatant was filtered and transferred to a new tube for subsequent injection and analysis by HPLC-Qtof-MS as described above.

Large-Scale ^{13}C-QmpA Reaction. The concentrations of all components were identical to those in the analytical-scale assays described above, but the total reaction volume was increased from 30 μL to 2.0 mL for the ^{13}C-QmpAsubstrate. Reactions were incubated for 16 h, quenched in the same manner as the small-scale reactions, and cleared by centrifugation and filtration.

Isolation of ^{13}C-QmpA Products from Large-Scale Reaction. Analytical HPLC was used to purify reacted ^{13}C-QmpA. The cleared filtrate was injected onto a Grace Vydac C18 column (5 μm, 250 × 4.6 mm) operating at 0.5 mL/min. Water and MeCN were used as mobile phases (both +0.1% FA). Elution was carried out with a gradient of 5−17.5% MeCN over 5 min, followed by a gradient from 17.5−100% over 25 min. The substrate and products coeluted at ∼22−23 min (∼70% MeCN). Fractions containing product were pooled, lyophilized, and assessed by HPLC−MS and NMR spectroscopy.

■ ASSOCIATED CONTENT

Supporting Information

The Supporting Information is available free of charge at https://pubs.acs.org/doi/10.1021/acs.joc.1c01507.

HR-MS and HR-MS/MS data for all substrates and products; UV−vis absorption spectrum of purified QmpB; 5′-deoxyadenosin formation assay; QmpB sequence comparison; 1D/2D NMR spectra of QmpB substrate and product (PDF)

■ AUTHOR INFORMATION

Corresponding Author

Mohammad R. Seyedsayamdost − *Department of Chemistry, Princeton University, Princeton, New Jersey 08544, United States; Department of Molecular Biology, Princeton University, Princeton, New Jersey 08544, United States;* orcid.org/0000-0003-2707-4854; Email: mrseyed@princeton.edu

Author

Alessio Caruso − *Department of Chemistry, Princeton University, Princeton, New Jersey 08544, United States*

Complete contact information is available at: https://pubs.acs.org/10.1021/acs.joc.1c01507

Notes

The authors declare no competing financial interest.

■ ACKNOWLEDGMENTS

We thank the National Science Foundation (NSF CAREER Award to M.R.S.) and the Eli Lilly-Edward C. Taylor Fellowship in Chemistry (to A.C.) for support of this work.

■ REFERENCES

(1) (a) Arnison, P. G.; Bibb, M. J.; Bierbaum, G.; Bowers, A. A.; Bugni, T. S.; Bulaj, G.; Camarero, J. A.; Campopiano, D. J.; Challis, G. L.; Clardy, J.; Cotter, P. D.; Craik, D. J.; Dawson, M.; Dittmann, E.; Donadio, S.; Dorrestein, P. C.; Entian, K.-D.; Fischbach, M. A.; Garavelli, J. S.; Göransson, U.; Gruber, C. W.; Haft, D. H.; Hemscheidt, T. K.; Hertweck, C.; Hill, C.; Horswill, A. R.; Jaspars, M.; Kelly, W. L.; Klinman, J. P.; Kuipers, O. P.; Link, A. J.; Liu, W.; Marahiel, M. A.; Mitchell, D. A.; Moll, G. N.; Moore, B. S.; Müller, R.; Nair, S. K.; Nes, I. F.; Norris, G. E.; Olivera, B. M.; Onaka, H.; Patchett, M. L.; Piel, J.; Reaney, M. J.; Rebuffat, S.; Ross, R. P.; Sahl, H.-G.; Schmidt, E. W.; Selsted, M. E.; Severinov, K.; Shen, B.; Sivonen, K.; Smith, L.; Stein, T.; Süssmuth, R. D.; Tagg, J. R.; Tang, G.-L.; Truman, A. W.; Vederas, J. C.; Walsh, C. T.; Walton, J. D.; Wenzel, S. C.; Willey, J. M.; van der Donk, W. A. Ribosomally synthesized and post-translationally modified peptide natural products: overview and recommendations for a universal nomenclature. *Nat. Prod. Rep.* **2013**, *30* (1), 108−160. (b) Hetrick, K. J.; van der Donk, W. A. Ribosomally synthesized and post-translationally modified peptide natural product discovery in the genomic era. *Curr. Opin. Chem. Biol.* **2017**, *38*, 36−44.

(2) Schramma, K. R.; Bushin, L. B.; Seyedsayamdost, M. R. Structure and biosynthesis of a macrocyclic peptide containing an unprecedented lysine-to-tryptophan crosslink. *Nat. Chem.* **2015**, *7* (5), 431−437.

(3) Isley, N. A.; Endo, Y.; Wu, Z.-C.; Covington, B. C.; Bushin, L. B.; Seyedsayamdost, M. R.; Boger, D. L. Total Synthesis and Stereochemical Assignment of Streptide. *J. Am. Chem. Soc.* **2019**, *141* (43), 17361−17369.

(4) (a) Frey, P. A.; Hegeman, A. D.; Ruzicka, F. J. The Radical SAM Superfamily. *Crit. Rev. Biochem. Mol. Biol.* **2008**, *43* (1), 63−88. (b) Landgraf, B. J.; McCarthy, E. L.; Booker, S. J. Radical *S*-Adenosylmethionine Enzymes in Human Health and Disease. *Annu. Rev. Biochem.* **2016**, *85* (1), 485−514. (c) Broderick, J. B.; Duffus, B. R.;

Duschene, K. S.; Shepard, E. M. Radical *S*-adenosylmethionine enzymes. *Chem. Rev.* **2014**, *114* (8), 4229−4317.
(5) Bushin, L. B.; Clark, K. A.; Pelczer, I.; Seyedsayamdost, M. R. Charting an Unexplored Streptococcal Biosynthetic Landscape Reveals a Unique Peptide Cyclization Motif. *J. Am. Chem. Soc.* **2018**, *140* (50), 17674−17684.
(6) (a) Ibrahim, M.; Guillot, A.; Wessner, F.; Algaron, F.; Besset, C.; Courtin, P.; Gardan, R.; Monnet, V. Control of the transcription of a short gene encoding a cyclic peptide in *Streptococcus thermophilus*: a new quorum-sensing system? *J. Bacteriol.* **2007**, *189* (24), 8844−8854. (b) Bassler, B. L.; Losick, R. Bacterially speaking. *Cell* **2006**, *125* (2), 237−246. (c) Jimenez, J. C.; Federle, M. J. Quorum sensing in group A Streptococcus. *Front. Cell. Infect. Microbiol.* **2014**, *4*, 127.
(7) Rued, B. E.; Covington, B. C.; Bushin, L. B.; Szewczyk, G.; Laczkovich, I.; Seyedsayamdost, M. R.; Federle, M. J. Quorum Sensing in *Streptococcus mutans* Regulates Production of Tryglysin, a Novel RaS-RiPP Antimicrobial Compound. *mBio* **2021**, *12* (2), e02688−20.
(8) Caruso, A.; Bushin, L. B.; Clark, K. A.; Martinie, R. J.; Seyedsayamdost, M. R. Radical Approach to Enzymatic β-Thioether Bond Formation. *J. Am. Chem. Soc.* **2019**, *141* (2), 990−997.
(9) Bushin, L. B.; Covington, B. C.; Rued, B. E.; Federle, M. J.; Seyedsayamdost, M. R. Discovery and Biosynthesis of Streptosactin, a Sactipeptide with an Alternative Topology Encoded by Commensal Bacteria in the Human Microbiome. *J. Am. Chem. Soc.* **2020**, *142* (38), 16265−16275.
(10) Clark, K. A.; Bushin, L. B.; Seyedsayamdost, M. R. Aliphatic Ether Bond Formation Expands the Scope of Radical SAM Enzymes in Natural Product Biosynthesis. *J. Am. Chem. Soc.* **2019**, *141* (27), 10610−10615.
(11) Caruso, A.; Martinie, R. J.; Bushin, L. B.; Seyedsayamdost, M. R. Macrocyclization via an Arginine-Tyrosine Crosslink Broadens the Reaction Scope of Radical *S*-Adenosylmethionine Enzymes. *J. Am. Chem. Soc.* **2019**, *141* (42), 16610−16614.
(12) (a) Lanz, N. D.; Grove, T. L.; Gogonea, C. B.; Lee, K.-H.; Krebs, C.; Booker, S. J. RlmN and AtsB as models for the overproduction and characterization of radical SAM proteins. *Methods Enzymol.* **2012**, *516*, 125−152. (b) Lanz, N. D.; Booker, S. J. Auxiliary iron-sulfur cofactors in radical SAM enzymes. *Biochim. Biophys. Acta, Mol. Cell Res.* **2015**, *1853* (6), 1316−1334.
(13) (a) Grell, T. A. J.; Goldman, P. J.; Drennan, C. L. SPASM and twitch domains in *S*-adenosylmethionine (SAM) radical enzymes. *J. Biol. Chem.* **2015**, *290* (7), 3964−3971. (b) Goldman, P. J.; Grove, T. L.; Booker, S. J.; Drennan, C. L. X-ray analysis of butirosin biosynthetic enzyme BtrN redefines structural motifs for AdoMet radical chemistry. *Proc. Natl. Acad. Sci. U. S. A.* **2013**, *110* (40), 15949−15954. (c) Davis, K. M.; Schramma, K. R.; Hansen, W. A.; Bacik, J. P.; Khare, S. D.; Seyedsayamdost, M. R.; Ando, N. Structures of the peptide-modifying radical SAM enzyme SuiB elucidate the basis of substrate recognition. *Proc. Natl. Acad. Sci. U. S. A.* **2017**, *114* (39), 10420−10425. (d) Grove, T. L.; Himes, P. M.; Hwang, S.; Yumerefendi, H.; Bonanno, J. B.; Kuhlman, B.; Almo, S. C.; Bowers, A. A. Structural Insights into Thioether Bond Formation in the Biosynthesis of Sactipeptides. *J. Am. Chem. Soc.* **2017**, *139* (34), 11734−11744.
(14) Hudson, G. A.; Burkhart, B. J.; DiCaprio, A. J.; Schwalen, C. J.; Kille, B.; Pogorelov, T. V.; Mitchell, D. A. Bioinformatic mapping of radical SAM-dependent RiPPs identifies new Cα, Cβ, and Cγ-linked thioether-containing peptides. *J. Am. Chem. Soc.* **2019**, *141* (20), 8228−8238.
(15) (a) Kawulka, K.; Sprules, T.; McKay, R. T.; Mercier, P.; Diaper, C. M.; Zuber, P.; Vederas, J. C. Structure of subtilosin A, an antimicrobial peptide from Bacillus subtilis with unusual posttranslational modifications linking cysteine sulfurs to alpha-carbons of phenylalanine and threonine. *J. Am. Chem. Soc.* **2003**, *125* (16), 4726−4727. (b) Kawulka, K. E.; Sprules, T.; Diaper, C. M.; Whittal, R. M.; McKay, R. T.; Mercier, P.; Zuber, P.; Vederas, J. C. Structure of Subtilosin A, a Cyclic Antimicrobial Peptide from Bacillus subtilis with Unusual Sulfur to alpha-Carbon Crosslinks: Formation and Reduction of alpha-Thio-alpha-Amino Acid Derivatives. *Biochemistry* **2004**, *43* (12), 3385−3395. (c) Liu, W.-T.; Yang, Y.-L.; Xu, Y.; Lamsa, A.; Haste, N. M.; Yang, J. Y.; Ng, J.; Gonzalez, D.; Ellermeier, C. D.; Straight, P. D.; Pevzner, P. A.; Pogliano, J.; Nizet, V.; Pogliano, K.; Dorrestein, P. C. Imaging mass spectrometry of intraspecies metabolic exchange revealed the cannibalistic factors of *Bacillus subtilis*. *Proc. Natl. Acad. Sci. U. S. A.* **2010**, *107* (37), 16286−16290. (d) Sit, C. S.; van Belkum, M. J.; McKay, R. T.; Worobo, R. W.; Vederas, J. C. The 3D solution structure of thurincin H, a bacteriocin with four sulfur to α-carbon crosslinks. *Angew. Chem., Int. Ed.* **2011**, *50* (37), 8718−8721.
(16) (a) Flühe, L.; Knappe, T. A.; Gattner, M. J.; Schäfer, A.; Burghaus, O.; Linne, U.; Marahiel, M. A. The radical SAM enzyme AlbA catalyzes thioether bond formation in subtilosin A. *Nat. Chem. Biol.* **2012**, *8* (4), 350−357. (b) Flühe, L.; Burghaus, O.; Wieckowski, B. M.; Giessen, T. W.; Linne, U.; Marahiel, M. A. Two [4Fe-4S] Clusters Containing Radical SAM Enzyme SkfB Catalyze Thioether Bond Formation during the Maturation of the Sporulation Killing Factor. *J. Am. Chem. Soc.* **2013**, *135* (3), 959−962. (c) Flühe, L.; Marahiel, M. A. Radical *S*-adenosylmethionine enzyme catalyzed thioether bond formation in sactipeptide biosynthesis. *Curr. Opin. Chem. Biol.* **2013**, *17* (4), 605−612. (d) Kincannon, W. M.; Bruender, N. A.; Bandarian, V. A Radical Clock Probe Uncouples H Atom Abstraction from Thioether Cross-Link Formation by the Radical *S*-Adenosyl-l-methionine Enzyme SkfB. *Biochemistry* **2018**, *57* (32), 4816−4823. (e) Grell, T. A. J.; Kincannon, W. M.; Bruender, N. A.; Blaesi, E. J.; Krebs, C.; Bandarian, V.; Drennan, C. L. Structural and spectroscopic analyses of the sporulation killing factor biosynthetic enzyme SkfB, a bacterial AdoMet radical sactisynthase. *J. Biol. Chem.* **2018**, *293* (45), 17349−17361.

https://doi.org/10.1021/acs.joc.1c01507
J. Org. Chem. 2021, 86, 11284−11289